



**HAL**  
open science

## Polyclonal expansion of TCR Vb 21.3 + CD4 + and CD8 + T cells is a hallmark of multisystem inflammatory syndrome in children

Marion Moreews, Kenz Le Gouge, Samira Khaldi-Plassart, Rémi Pescarmona, Anne-Laure Mathieu, Christophe Malcus, Sophia Djebali, Alicia Bellomo, Olivier Dauwalder, Magali Perret, et al.

### ► To cite this version:

Marion Moreews, Kenz Le Gouge, Samira Khaldi-Plassart, Rémi Pescarmona, Anne-Laure Mathieu, et al.. Polyclonal expansion of TCR Vb 21.3 + CD4 + and CD8 + T cells is a hallmark of multisystem inflammatory syndrome in children. *Science Immunology*, 2021, 6 (59), pp.eabh1516. 10.1126/sciimmunol.abh1516 . hal-03298662

**HAL Id: hal-03298662**

**<https://hal.science/hal-03298662>**

Submitted on 9 Jan 2024

**HAL** is a multi-disciplinary open access archive for the deposit and dissemination of scientific research documents, whether they are published or not. The documents may come from teaching and research institutions in France or abroad, or from public or private research centers.

L'archive ouverte pluridisciplinaire **HAL**, est destinée au dépôt et à la diffusion de documents scientifiques de niveau recherche, publiés ou non, émanant des établissements d'enseignement et de recherche français ou étrangers, des laboratoires publics ou privés.

## Polyclonal expansion of TCR Vbeta 21.3+ CD4+ and CD8+ T cells is a hallmark of Multisystem Inflammatory Syndrome in Children

Marion Moreews<sup>1</sup>, Kenz Le Gouge<sup>2,\*</sup>, Samira Khaldi-Plassart<sup>3,4,\*</sup>, Rémi Pescarmona<sup>1,4,5,\*</sup>, Anne-Laure Mathieu<sup>1,\*</sup>, Christophe Malcus<sup>6,7</sup>, Sophia Djebali<sup>1</sup>, Alicia Bellomo<sup>1</sup>, Olivier Dauwalder<sup>1,8</sup>, Magali Perret<sup>1,5</sup>, Marine Villard<sup>1,5</sup>, Emilie Chopin<sup>9</sup>, Isabelle Rouvet<sup>9</sup>, Francois Vandenesch<sup>1,8</sup>, Céline Dupieux<sup>1,8</sup>, Robin Pouyau<sup>10</sup>, Sonia Teysse<sup>10</sup>, Margaux Guerder<sup>10</sup>, Tiphaine Louazon<sup>11</sup>, Anne-Moulin-Zinsch<sup>12</sup>, Marie Duperril<sup>13</sup>, Hugues Patural<sup>13,14</sup>, Lisa Giovannini-Chami<sup>15,16</sup>, Aurélie Portefaix<sup>17</sup>, Behrouz Kassai<sup>17</sup>, Fabienne Venet<sup>1,6</sup>, Guillaume Monneret<sup>6,7</sup>, Christine Lombard<sup>5</sup>, Hugues Flodrops<sup>18</sup>, Jean-Marie De Guillebon<sup>19</sup>, Fanny Bajolle<sup>20</sup>, Valérie Launay<sup>21</sup>, Paul Bastard<sup>22,23</sup>, Shen-Ying Zhang<sup>22,23,24</sup>, Valérie Dubois<sup>25</sup>, Olivier Thauinat<sup>1,25,26,27</sup>, Jean-Christophe Richard<sup>28,29</sup>, Mehdi Mezidi<sup>28,29</sup>, Omran Allatif<sup>1</sup>, Kahina Saker<sup>1,30</sup>, Marlène Dreux<sup>1</sup>, Laurent Abel<sup>22,23,24</sup>, Jean-Laurent Casanova<sup>22,23,24,31</sup>, Jacqueline Marvel<sup>1</sup>, Sophie Trouillet-Assant<sup>1,30</sup>, David Klatzmann<sup>2,32</sup>, Thierry Walzer<sup>\*,1</sup>, Encarnita Mariotti-Ferrandiz<sup>\*,2,32</sup>, Etienne Javouhey<sup>\*,7,10</sup>, Alexandre Belot<sup>1,6</sup>

<sup>1</sup>CIRI, Centre International de Recherche en Infectiologie, Univ Lyon, Inserm, U1111, Université Claude Bernard, Lyon 1, CNRS, UMR5308, ENS de Lyon, F-69007, Lyon, France

<sup>2</sup>Sorbonne Université, UPMC Univ Paris 06, INSERM UMRS 959, Immunology Immunopathology-Immunotherapy (i3), Paris, France

<sup>3</sup>(RAISE), France; Pediatric Nephrology, Rheumatology, Dermatology Unit, Hôpital Femme Mère Enfant, Hospices Civils de Lyon

<sup>4</sup>National Referee Centre for Rheumatic and AutoImmune and Systemic diseases in childrEn

<sup>5</sup>Immunology Laboratory, Hospices Civils de Lyon, Lyon Sud Hospital, Pierre-Bénite

<sup>6</sup>Hospices Civils de Lyon, Edouard Herriot Hospital, Immunology Laboratory, 69437 Lyon, France

<sup>7</sup>EA 7426 "Pathophysiology of Injury-Induced Immunosuppression" (Université Claude Bernard Lyon 1 - Hospices Civils de Lyon - bioMérieux), Joint Research Unit HCL-bioMérieux, 69003, Lyon, France

**Corresponding author:** Pr Alexandre Belot, CIRI, Centre International de Recherche en Infectiologie, Univ Lyon, Inserm, U1111, Université Claude Bernard, Lyon 1, CNRS, UMR5308, ENS de Lyon, F-69007, Lyon, France & National Referee Centre for Rheumatic and AutoImmune and Systemic diseases in childrEn (RAISE), France; Pediatric Nephrology, Rheumatology, Dermatology Unit, Hôpital Femme Mère Enfant, Hospices Civils de Lyon, France, alexandre.belot@chu-lyon.fr.  
\*equal contribution

**Author contributions:** AB, TW, DK, JM, EM-F designed and analyzed experiments MM, K LG, AB, CM, RP, SP, SJ, ALM, MP, MV, EC, IR, FV, PB, SYZ performed and analyzed experiments. CM, GM and FV conceptualized the FACS analysis CM and RP supervised cytokine experiments. EJ performed inclusions, chair the clinical investigation and took care of all ethical committee agreement. AP, YJ and BK set up the clinical, RP, ST, MG, TL, FV, AMZ, MD, HP, LC, JCR, MM, OD, JMDG, FB provided clinical samples and clinical details for all cohorts. OT and VB explored HLA in MIS-C patients and JLC, LA supervised genetic inference exploration of HLA. IR and EC provided biobanking and help to generate material for the study TW and AB supervised, designed and funded this study. TW and AB prepared the initial draft. All authors critically reviewed the paper and agreed on the final form.

This work is dedicated to the memory of Dr Tomisaku Kawasaki.

**Competing interests:** The authors have no competing interests.

**Data and materials availability:** All information and data are available upon request

- <sup>8</sup>Centre National de Référence des Staphylocoques, Institut des Agents Infectieux, Hospices Civils de Lyon, F-69004, Lyon, France
- <sup>9</sup>Cellular Biotechnology Department and Biobank, Hospices Civils de Lyon, Lyon, France
- <sup>10</sup>Réanimation Pédiatrique Hôpital Femme-Mère-Enfant Hospices Civils de Lyon, Bron, France
- <sup>11</sup>Service de pédiatrie, Centre Hospitalier de Valence, France
- <sup>12</sup>Unité medico-chirurgicale des cardiopathies congénitales, hôpital Louis-Pradel, hospices civils de Lyon, 69677 Bron, France.
- <sup>13</sup>Pediatric intensive care unit - University hospital of Saint-Étienne, France
- <sup>14</sup>U1059 INSERM - SAINBIOSE - DVH – Université de Saint-Étienne – 42055, France
- <sup>15</sup>Pediatric Pulmonology and Allergology Department, Hôpitaux pédiatriques de Nice CHU-Lenval, Nice, France
- <sup>16</sup>Université Côte d'Azur, France
- <sup>17</sup>Center of Clinical Investigation, Lyon University Hospital, Bron, France
- <sup>18</sup>Service de Pédiatrie, Groupe Hospitalier Sud Réunion, CHU de La Réunion, Saint Pierre, La Réunion, France.
- <sup>19</sup>Service de Néphrologie, Rhumatologie pédiatrique, Hôpitaux pédiatriques de Nice CHU-Lenval, Nice, France
- <sup>20</sup>Hôpital Necker Enfants Malades, Centre de référence M3C, AP-HP, Paris, France
- <sup>21</sup>Urgences pédiatriques , Hôpital femme Mère Enfant, Hospices Civils de Lyon, Bron, France
- <sup>22</sup>Laboratory of Human Genetics of Infectious Diseases, Necker Branch, INSERM U1163, Necker Hospital for Sick Children, Paris, France.
- <sup>23</sup>University of Paris, Imagine Institute, Paris, France
- <sup>24</sup>St. Giles Laboratory of Human Genetics of Infectious Diseases, Rockefeller Branch, The Rockefeller University, New York, NY, USA
- <sup>25</sup>EFS Auvergne Rhône Alpes, laboratoire Histocompatibilité, 111, rue Elisée-Reclus, 69150 Décines, France
- <sup>26</sup>Department of Transplantation, Nephrology and Clinical Immunology, Edouard Herriot University Hospital, Lyon, France;
- <sup>27</sup>Lyon-Est Medical Faculty, Claude Bernard University (Lyon 1), 8, avenue Rockefeller, 69373, Lyon, France.
- <sup>28</sup>Médecine Intensive-Réanimation, Hôpital de la Croix-Rousse, Hospices Civils de Lyon, Lyon, France
- <sup>29</sup>Lyon University, France;
- <sup>30</sup>Laboratoire de Virologie, Institut des Agents Infectieux, Laboratoire associé au Centre National de Référence des virus des infections respiratoires, Hospices Civils de Lyon, Lyon, France

<sup>31</sup>Howard Hughes Medical Institute, NY, USA

<sup>32</sup>Assistance Publique - Hôpitaux de Paris, Hôpital Pitié-Salpêtrière, Biotherapy and Département Hospitalo-Universitaire Inflammation-Immunopathology-Biotherapy (i2B), Paris, France.

## Abstract

**Objectives**—Multiple Inflammatory Syndrome in Children (MIS-C) is a delayed and severe complication of SARS-CoV-2 infection that strikes previously healthy children. As MIS-C combines clinical features of Kawasaki disease and Toxic Shock Syndrome (TSS), we aimed to compare the immunological profile of pediatric patients with these different conditions.

**Methods**—We analyzed blood cytokine expression and T cell repertoire and phenotype in 36 MIS-C cases in comparison with 16 KD, 58 TSS, and 42 COVID-19 cases.

**Results**—Similarly to TSS, an increase of serum inflammatory cytokines (IL-6, IL-10, IL-18, TNF- $\alpha$ , IFN $\gamma$ , CD25s, MCP1, IL-1RA) was observed in MIS-C contrasting with low expression of HLA-DR in monocytes. A specific expansion of T cells with an activated phenotype and expressing the V $\beta$ 21.3 T cell receptor  $\beta$  chain variable region and correlating with the cytokine storm was detected in both CD4 and CD8 subsets in 75% of MIS-C patients and not in any patient with TSS, KD, or acute COVID-19. TCR sequencing uncovered the polyclonal nature of the V $\beta$  21.3+ population. The T cell repertoire returned to normal within weeks after MIS-C resolution. V $\beta$ 21.3+ T cells from MIS-C patients expressed high levels of HLA-DR, CD38 and CX3CR1 but did not react against SARS-CoV-2 peptides *in vitro* unlike T cells from COVID-19 patients. Consistently, the T cell expansion was not associated with specific classical HLA alleles.

**Conclusions:** We demonstrate the existence of a specific polyclonal V $\beta$ 21.3 T cell expansion in MIS-C patients not directed against SARS-CoV-2 antigenic peptides and not observed in other related conditions, namely KD, TSS and acute COVID-19.

## One Sentence Summary:

We report the expansion of a polyclonal and activated TCR V $\beta$ 21.3+ subset of CD4+ and CD8+ T cells in about 75% of MIS-C patients, which are not specific of HLA-restricted SARS-CoV-2 antigenic peptides and not observed in Kawasaki disease and toxic shock syndrome.

## Keywords

MIS-C; PIMS; COVID-19; SARS-CoV2; post-infectious disease; Kawasaki disease; Toxic Shock Syndrome; Immune profiling; TCR sequencing; myocarditis

## Introduction

At the end of April 2020, European clinicians warned the Public Health Agencies about an abnormal increase of Kawasaki-like diseases (KLD) and myocarditis requiring critical care support in the context of the ongoing COVID-19 epidemic in children (1-3). Later on, American clinicians also reported a large outbreak of severe inflammation in children following COVID-19 infection, a condition that is now named Pediatric Inflammatory Multisystemic Syndrome (PIMS) or Multisystem Inflammatory Syndrome in children (MIS-

C) (4-6). The clinical phenotype of this emerging disease is broad and encompasses features of Kawasaki disease (KD) and toxic shock syndrome (TSS). Many cases require intensive care support, making MIS-C one of the most severe manifestation of COVID-19 in children. Of note, the temporal occurrence of MIS-C raised the hypothesis of a post-infectious disease occurring about 3 to 4 weeks after acute COVID-19 in children (3, 5-7).

To date, reports on MIS-C have shown slight differences in cytokine profiling and immunophenotype between MIS-C and KD or pediatric COVID-19 (8, 9). Analysis of T cells revealed a lower number of T cells in MIS-C with no or subtle signs of activation (10). Multi-dimensional immune profiling on small numbers of patients showed differences between acute COVID-19 or pre-pandemic KD (8, 11). Anti-SARS-CoV2 antibodies were equally produced in pediatric COVID-19 and MIS-C. Autoantibodies were uniquely found during MIS-C or KD, which supports a contribution of the humoral response to both diseases (8, 11). Finally, a role for genetic factors has been evocated in MIS-C pathogenesis as it seems to occur more frequently in children from Hispanic or African ethnicity (12-14). Despite these pioneer studies, the immunological mechanism underlying MIS-C remains unknown.

To address this question, we compared the immune profile in MIS-C patients in comparison to that of COVID-19 patients and that of patients with other clinically similar entities such as KD and TSS. For this, we explored the cytokine and cellular immune profile using different techniques. Using flow cytometry and transcriptomic analyses, we uncovered a specific V $\beta$ 21.3+ T cell expansion in 24/32 tested patients in MIS-C patients when assessed in the first month after onset. TCR sequencing revealed the polyclonal nature of the V $\beta$ 21.3+ expansion. No specific HLA bias was identified in patients but we found a specific activation profile within V $\beta$ 21.3+ T cells. This activation was transient with a normalization of the repertoire within days to weeks after the inflammatory episode.

## Results:

### MIS-C presentation overlaps with TSS and KD

We constituted a cohort of 36 children with MIS-C and compared them with 16 KD diagnosed during and before the pandemic, 58 retrospective cases of TSS patients and 42 patients with acute COVID-19 (11 children, 31 adults). This comparison was motivated by previous descriptions of MIS-C in Europe and in the US, showing a clinical overlap between staphylococcal toxin-mediated TSS and KD in patients with MIS-C. Figure 1A outlines the study flowchart and the clinical and biological parameters we evaluated. Patients included fulfilled criteria for MIS-C, classical KD or TSS. All three groups of patients were then subjected to deep immunological analyses combining cytokine profiling, TCR V $\beta$  analysis and T cell stimulation assays (Fig. 1A). We confirmed the strong clinical overlap between MIS-C, TSS and KD. Indeed, many patients in the MIS-C group fulfilled the major criteria for TSS and KD respectively (Fig. 1B). Considering the clinical parameters, the most frequent features of MIS-C patients in our cohort were fever, cardiac dysfunction, gastrointestinal symptoms, coagulopathy and systemic inflammation (Fig. 1C). Additional clinical data are presented in Table 1 for KD, TSS and acute COVID-19., and in Table S1 for

all patients. Moreover, Table S2 gives a list of the patients analyzed in each of the following figure panels.

### **High levels of proinflammatory cytokines in MIS-C contrasting with lymphopenia and low HLA-DR expression in monocytes.**

SARS-CoV2 can cause fatal acute respiratory distress syndrome in patients at risk. This manifestation is caused by delayed and poorly controlled immune responses, with a deleterious role of inflammatory cytokines. Moreover, we and others have identified a subgroup of severe COVID-19 patients with impaired type-I interferon production (15-18). Thus a regulated production of cytokines is paramount for a good control of SARS-CoV2 infection. This prompted us to investigate how cytokines could contribute to MIS-C pathogenesis. We compared the serum level of IFN- $\alpha$ , IFN- $\gamma$ , TNF- $\alpha$ , IL-10, soluble CD25 (sCD25), MCP1, IL1Ra, IL-6 and IL-18 between healthy controls and MIS-C, KD, TSS and different forms of COVID-19 (mild pediatric, mild or severe adult-onset COVID-19, see Table S1 for a list of clinical features in the different patients' groups).

The expression of interferon-stimulated genes (ISGs) in blood cells was significantly higher in MIS-C compared to controls, but rather low compared to COVID-19 patients (Fig. 2A). The level of serum IFN $\alpha$ 2 followed the same trends, while serum IFN $\gamma$  was variable among MIS-C patients, with very high levels in a few patients. The expression of the other cytokines measured (IL-6, IL-10, IL-18, TNF $\alpha$ , MCP1, IL1RA, CD25s) was very high in MIS-C patients compared to controls, and very similar to that of KD, TSS and severe COVID-19 patients (Fig. 2B-C). Of note the level of CD25s was significantly higher in TSS than in MIS-C patients, and significantly lower in severe COVID-19 patients than in MIS-C patients (Fig. 2B-C). Of note, a previous study found higher levels of serum IL-6 in KD patients than in MIS-C contrasting with our data (8).

To further explore the MIS-C immunological profile, we then quantified the number of peripheral lymphocytes of different types, as well as the expression of HLA-DR in patient's monocytes. T and NK cell counts were on average very low in MIS-C and KD patients while B cell counts were normal (Fig. 2D). We found a decreased expression of HLA-DR in monocytes in both KD and MIS-C patients compared to controls (Fig. 2E). Altogether our data show a strong similarity in cytokine profiles between MIS-C, KD and TSS and highlight the decreased lymphocyte counts and low HLA-DR expression in monocytes in MIS-C patients compared to controls.

### **Expansion of V $\beta$ 21.3+ peripheral T cells in a large fraction of MIS-C patients**

TSST1-related TSS is associated with a skewing of the T cell repertoire towards V $\beta$ 2, as a result of TSST1-superantigen induced proliferation of V $\beta$ 2+ T cells (19). Every other *S. aureus* superantigenic toxins induce the expansion of specific TCR V $\beta$  subsets, i.e. V $\beta$  5.2, 5.3, 7.2, 9, 16, 18, 22 for staphylococcal enterotoxin A (SEA) or V $\beta$  3, 12, 13.2, 14, 17, 20 for SEB (20). Given the similarities between TSS and MIS-C, we explored the possibility that MIS-C was also associated with specific T cell expansions. To explore the T cell repertoire in MIS-C, we first used flow cytometry to assess the distribution of V $\beta$  subunits in T cells from MIS-C patients, in comparison with KD, TSS and COVID-19

patients (Fig. 3A). As expected, TSS patients displayed the hallmark expansion of the V $\beta$ 2+ subset. Interestingly, several V $\beta$ -specific expansions were also visible in MIS-C patients, and in most cases V $\beta$ 21.3+ expansions (Fig. 3A), in both CD4 and CD8 T subsets (Fig. S1A-B). These expansions had similar amplitudes as the V $\beta$ 2+ expansions in TSS (Fig. 3A). A principal component analysis of the V $\beta$  distribution in CD4 and CD8 T cells showed that the main parameters separating the different patients were the frequency of V $\beta$ 2+ and the frequency of V $\beta$ 21.3+ cells (Fig. S1C-D). Overall, the expansion of V $\beta$ 21.3+ T cell subsets was seen in 15/26 (58%) of MIS-C patients and in none of the other conditions analyzed by flow cytometry ie KD, TSS and COVID-19 (Fig. 3A). Next, we wanted to use a different technique to test the specificity of this expansion, and we therefore performed transcriptomic analyses of V $\beta$  expression in PBMC using the Nanostring technology. This technique also requires much less material than flow cytometry, which allowed us to run lymphopenic samples from severe COVID-19 cases. This transcriptomic analysis firmly established that the V $\beta$ 21.3+ T cell expansion is a hallmark of MIS-C as it was seen in 18/23 MIS-C patients tested (Fig. S1E). Thus, taking together flow cytometry and Nanostring analyses, we found that 24/32 (75%) of MIS-C patients and none in the other clinical groups displayed *TRBV11-2*/V $\beta$ 21.3+ expansions.

In an effort to understand the physiopathological mechanism underlying MIS-C we then compared the level of serum cytokines between MIS-C patients with and without V $\beta$ 21.3+ T cell expansions, at the time of the acute episode. The levels of IL-18 and IL-1RA (Fig. 3C-D) were associated with the expansions, but not those of the other cytokines tested (Fig. S2B), suggesting that V $\beta$ 21.3+ T cells were associated with the cytokine storm.

### TCR sequencing highlights the polyclonal nature of TCR V $\beta$ 21.3 expansions

To investigate the clonality of V $\beta$ 21.3+ expanded cells, we analyzed the TCR repertoire of 11 MIS-C patients for whom whole blood RNA was available by TCR-sequencing. We analyzed the composition of the TCR beta rearrangements involving the *TRBV11-2* gene (which corresponds to V $\beta$ 21.3). First, by representing the *TRBV11-2*/*TRBJ* combination usage as chord diagrams (Fig. 3E, 3F), we confirmed the expansion of T cells using *TRBV11-2* in 7 out of the 11 patients (MIS-C-3, 7, 8, 9, 13, 23, 26). These *TRBV11-2* rearrangements were associated with multiple *TRBJ* genes, suggesting the polyclonal nature of the expansions. To further evaluate the polyclonality, we analyzed the CDR3 length distribution of *TRBV11-2* clonotypes (barplots Fig. 3E-F-G.). The CDR3 spectratype distributions are typical of the bell-shaped Gaussian distribution expected in polyclonal repertoires. In order to evaluate the degree of polyclonality, we identified the expanded clonotypes by setting a threshold based on the binomial distribution of the clonotype frequencies per sample (see methods section and Fig. S3A). No major monoclonal expansions (red lines in the CDR3 spectratypes) explaining the global *TRBV11-2* expansion were detected. Instead, most of the clonotypes were found at low frequencies (grey lines), typical of a polyclonal diverse repertoire. The percentages of expanded clonotypes were not significantly different between patients with or without *TRBV11-2*. We calculated the cumulative frequencies of such expanded clonotypes within the full repertoire and found that they were always far below the frequency of the full *TRBV11-2* expansion in patients with expansions, representing in average 0,51 % of the total repertoire. Finally, these limited

expansions represented in average 4,47% of the TRBV11-2 repertoire in patients with TRBV11-2 expansions and 6,31% in patients without TRBV11-2 expansions (Table S4 and Fig. S3B). To confirm the polyclonality of the TRBV11-2 expansion, we computed the Berger-Parker index (BPI) on TRBV11-2 clonotype for MIS-C patients harboring or not TRBV11-2 expansions (Fig. S3C). This index measures the proportional abundance of the most abundant clonotypes within TRBV11-2 clonotypes. There was no significant differences when we compared the BPI on TRBV11-2 clonotypes between patients with or without TRBV11-2 expansions, further confirming that TRBV11-2 expansions in the 7 patients are not explained by monoclonal expansions.

We then asked whether the V $\beta$ 21.3+ T cell expansion persisted overtime. For this we repeated the TCR sequencing and the flow cytometry V $\beta$  analyses in a group of patients for which blood samples were available during and after the acute inflammatory episode. As shown in Figures 3F-H, the V $\beta$ 21.3/TRBV11-2 distributions for all the patients returned to normal within days to weeks after MIS-C. Interestingly, when we compared the CDR3 length distributions by calculating the perturbation score using the ISEApeaks tool between repertoires obtained during and after the acute response, we found no differences between the two groups, further supporting the polyclonal expansion profile of TRBV11-2 during the acute response (Fig. S3D). Finally, this transient expansion suggested a pro-apoptotic phenotype of V $\beta$ 21.3+ T cell. To test this hypothesis, we stained PBMCs from MIS-C patients with Annexin-V that marks early apoptotic cells. A higher fraction of V $\beta$ 21.3+ compared with V $\beta$ 21.3-T cells were stained with Annexin-V in MIS-C patients with V $\beta$ 21.3+ expansions (Fig. 3I), which substantiated our hypothesis.

### **V $\beta$ 21.3+ T cells have an activated phenotype but do not react against SARS-CoV2 peptides**

As V $\beta$ 21.3+ T cells expand in MIS-C patients, we investigated their activation status and the mechanisms underlying their proliferation. We found that the activation markers HLA-DR and CD38 were expressed at high levels in both CD4 and CD8 T cells from MIS-C patients with V $\beta$ 21.3+ expansions compared to those without expansions and to healthy controls (Fig. 4A-4B). This was due to a specific up regulation of CD38 and HLA-DR in V $\beta$ 21.3+ CD4 and CD8 T cells in MIS-C patients with expansions compared to those without expansions (Fig. 4C, 4D). A recent paper reported a specific activation of CX3CR1+ CD4 and CD8 T cells in MIS-C patients, as assessed by HLA-DR/CD38 levels(22). This prompted us to measure CX3CR1 levels in V $\beta$ 21.3+ T cells. As shown in Figure 4E, V $\beta$ 21.3+ were in majority CX3CR1 positive both in CD4 and CD8 T cells in MIS-C patients with V $\beta$ 21.3+ expansions compared to those without expansions, even though the percentage of CX3CR1 positive cells was not higher in MIS-C than in control patients (Fig. S4A). Moreover, in MIS-C patients, a large frequency of CX3CR1+ CD4 and CD8 T cells had an activated phenotype in terms of HLA-DR and CD38 expression (Fig. S4B).

Given that MIS-C followed COVID-19, we wondered if V $\beta$ 21.3+ T cells were raised against SARS-CoV-2 antigens. To test this possibility, we stimulated PBMCs from MIS-C or convalescent COVID-19 patients with a commercial cocktail of SARS-CoV2 peptides spanning S, N and M viral proteins. T cells from MIS-C patients responded poorly to stimulation with viral peptides, regardless of V $\beta$ 21.3 expansion, compared to T cells from



convalescent COVID-19 patients that responded well (Fig. 4F, 4E, S3). This was not due to a lack of adaptive anti-SARS-CoV-2 response, because all MIS-C patients tested had high SARS-CoV-2-specific antibody levels (Fig. S4C-E). Finally, we could not identify any specific allele nor mutations of classical HLA class I or class II genes associated with TRBV11-2 expansions by genomic sequencing of the HLA loci of 13 MIS-C patients (Table S3). Together with the lack of V $\beta$ 21.3+ expansion in COVID-19 patients, these data show that V $\beta$ 21.3+ T cells are not specific for HLA-restricted SARS-CoV-2 peptides.

## Discussion

Here, we first confirmed the strong overlap in clinical phenotype between KD, MIS-C, and TSS. MIS-C and TSS were even more similar to each other with cardiac dysfunction, hypotension, maculo-papular skin rash and conjunctivitis as defining features. Moreover, we have recently identified the critical importance of early steroid therapy in the management of MIS-C, similarly to what has been previously shown in TSS (23, 24). MIS-C and TSS are obviously linked to infections, while many KD features suggest an infectious cause for KD as well (25). In particular, the efficacy of IV immunoglobulins, the occurrence in young children, the acute nature of the disease and the absence of relapse suggest that an infectious agent is driving the pathogenesis. The epidemic of a novel coronavirus in 2005 (New Haven) was associated to KD and linked the viral infection to vascular inflammation(26).

We found important similarities in terms of cytokine expression between MIS-C, TSS and KD such as high TNF- $\alpha$ , IL6, IL18 and IL1Ra levels. A previous study noted that a subgroup of severe MIS-C patients had higher levels of IFN- $\gamma$ , IL-18, GM-CSF, RANTES, IP-10, IL-1 $\alpha$ , and SDF-1 than mild MIS-C or KD patients (27). We also observed a subset of MIS-C patients with high serum IFN- $\gamma$ , IL-18 and CD25s. These observations confirm previous reports showing a clinical and biological overlap between MIS-C and macrophage activation syndrome(3), and suggest the importance of IFN- $\gamma$  in the disease. The suppressor of cytokine signaling protein-1 SOCS1 is a major negative regulator of IFN- $\gamma$  signaling and SOCS1 haploinsufficiency is associated to an increase of IFN- $\gamma$  sensitivity(28, 29). A recent paper reported MIS-C development in a child with heterozygous loss-of-function SOCS1 mutations (1), perhaps suggesting a pathological role for IFN- $\gamma$ . However there are also important differences between immune profiles of MIS-C and hemophagocytic syndrome. Indeed, the latter is characterized by very high HLA-DR expression in monocytes (30) while we observed low expression of HLA-DR in monocytes in MIS-C patients. This observation is suggestive of immune unresponsiveness, as seen following TSS or septic shock (30-33). Indeed, low HLA-DR expression in monocytes is considered as a very good marker of sepsis-induced immunosuppression (33).

We report the expansion of a TCR V $\beta$ 21.3+ T cell subset with an activated phenotype in as many as 75% of MIS-C patients. These expansions were identified using flow cytometry experiments taking advantage of available antibodies against the different V $\beta$  chains, and with a new dedicated Nanostring panel allowing the measurement of mRNA encoding for these chains in whole blood in a large number of MIS-C patients. V $\beta$ 21.3+ T cell expansions were also reported in smaller numbers of MIS-C patients in two recent studies, that used either TCR sequencing or single cell RNA-seq (34, 35). In both Porritt and our study

V $\beta$ 21.3+ T cell expansions appeared polyclonal as judged by the large number of TRBJ gene segments associated with TRBV11.2 and by the even distribution of the CDR3 domain. Our study is however the only one to show that V $\beta$ 21.3+ CD4 and CD8 T cell expansions are a feature of MIS-C that well discriminates them from KD, TSS and COVID-19 patients.

We observed a correlation between V $\beta$ 21.3+ T cell expansions and the level of serum cytokines IL-18 and IL-1RA from matching samples, confirming a previous study (36) and indicating that V $\beta$ 21.3+ T cell expansions are associated with the cytokine storm. Our data also show that V $\beta$ 21.3+ T cells have an activated phenotype, with high HLA-DR and CD38 expression and that activated V $\beta$ 21.3+ T cells expressed high levels of CX3CR1, a marker of patrolling monocytes and of cytotoxic lymphocytes. CX3CR1 binds to CX3CL1, a membrane-bound chemokine induced on vascular endothelial cells upon inflammation. The CX3CL1-CX3CR1 axis is thought to have an important role in vascular inflammation in different inflammatory diseases(37), and could contribute to MIS-C pathogenesis. This interaction could promote the cytotoxic action of different lymphocyte populations, which fits with the reported elevated expression of cytotoxicity genes in NK and CD8+ T cells in MIS-C patients(38).

We demonstrate that both TSS and MIS-C are marked by the polyclonal proliferation of a specific V $\beta$  subset i.e. V $\beta$ 2+ cells for TSS related to TSST1, and V $\beta$ 21.3+ cells for MIS-C. We found that the amplitude of the expansion was also similar in both syndromes. Considering the other similarities between MIS-C and TSS shown in this study in terms of clinical phenotype, cytokine production and treatment, this raises the hypothesis that V $\beta$ 21.3+ cell expansions are caused by a superantigen structure in MIS-C. The term superantigen has been coined by Kappler and Marrack as an operational definition of various T-cell activating substances with specificity for T cell antigen receptors V $\beta$  subunits regardless of the rearrangement and antigen-specificity (39). Superantigens bind external regions of T cell receptor and MHC molecules (40) and can induce massive expansions of T cells expressing one specific TCR V $\beta$  chain while classical antigens induce the expansion of T cells bearing different V $\beta$ . Previous papers have suggested that the SARS-CoV2 Spike protein could behave as a superantigen structure (41). Using *in silico* modelling, Porritt et al identified a putative interaction between V $\beta$ 21.3 and a superantigen-like motif on the spike of SARS-CoV2. However, V $\beta$ 21.3+ T cell expansions occur in a delayed manner relative to SARS-CoV-2 infection, and the virus is often undetectable in MIS-C patients at the time of the acute inflammation. The kinetics of MIS-C relative to COVID-19 is compatible with a causal role of anti-SARS-CoV-2 antibodies. One can hypothesize that immune complexes composed of SARS-CoV-2 bound to antibodies may act as superantigen structures. However, a previous study failed to detect such immune complexes in MIS-C patients(27). In addition, V $\beta$  restricted T cells have been shown to adhere to endothelial cells following superantigen activation(42) and thus the CX3CR1+ V $\beta$ 21.3 expanded T cells may play a role in vascular injury in MIS-C. Alternative mechanisms may be put forward, such as secondary autoimmune reactions. Several studies have indeed reported the appearance of autoantibodies in MIS-C patients, some of which directed against endothelial antigens(8, 11), while others have reported immune events consistent with autoimmunity such as the expansion of proliferating plasmablasts(38) or the persistence of functional SARS-CoV-2-specific monocyte-activating antibodies(43). How B cell mediated autoimmunity would

be linked to V $\beta$  specific T cell expansions is however unclear. One could speculate that immune complexes composed of autoantibodies and endogenous antigens could behave as superantigens. Finally, given the rarity of MIS-C, there could be a genetic susceptibility to this post-infectious disease promoting hyperinflammatory reaction of adaptive immunity in response to SARS-CoV2(14). We limited our analysis to classical HLA alleles, but did not find any significant association, even though a previous study reported an HLA-I bias in a smallest group of MIS-C patients(36).

### Limitations of the study:

All samples from MIS-C patients were obtained after anti-inflammatory treatments (see supplementary table I), and it is likely that those treatments affect the level of serum cytokines, which could have impacted the comparisons we made between clinical conditions, and the associations between cytokines and T cell expansions.

## Methods

### Study design

The aim of the study was to compare MIS-C features with those of Kawasaki disease and Toxic Shock Syndrome (TSS). The immunological profile of 36 MIS-C cases, 16 KD and 58 TSS cases and 42 non-MISC COVID-19 were included (Fig. 1A). Samples were collected within the first week of symptoms and analyzed for cytokine immunoprofiling, standard immunophenotyping, V $\beta$  expression, TCR sequencing, SARS-CoV2-dependent T cell response. Because of low volume sampling of pediatric patients, we did not have the same availability for research blood draws. The samples used for each experiments are detailed in table S2.

### Patients and ethics

Four distinct cohorts were used for the data collection and analyses registered in [ClinicalTrial.gov](https://www.clinicaltrials.gov) and consents were obtained from parents. The main clinical features are summarized in Fig. 1C, Table 1, Table S2. Written informed consent was obtained for all data collection and blood sampling as detailed in supplemental material. The 36 MIS-C patients were included since the beginning of the pandemics, from April 2020 from French participating centers (HPI COVID). We took advantage of previous collection of Kawasaki from Necker's Hospital and additional patients with KD or TSS previously included into a study on toxic shock syndrome (approved by the Ethical review board Sud Est IV, DC-2008-176). Acute COVID-19 patients were derived from either HPI project on pediatric COVID-19 (HPI COVID), n=11 or from two ongoing project on mild adult COVID-19 in health care providers (COVID-SER), n=21 or severe adult COVID-19 in critical care unit (COVID-Rea), n=10. All details for ethical agreement are listed in Supplemental material. Clinical information of KD, COVID-19 and TSS patients are detailed in Table 2 and Table S2. All patients could not be included in all analysis, this information is provided in Table S1.

### Cytokines and IFN score assessment

Whole blood was sampled on EDTA tubes and plasma was frozen at  $-20^{\circ}\text{C}$  within 4 hours following blood collection. Plasma concentrations of IL-6, TNF- $\alpha$ , IFN- $\gamma$ , IL-10, MCP-1, IL-1ra and CD25s were measured by Simpleplex technology using ELLA instrument (ProteinSimple), following manufacturer's instructions. Plasma IFN- $\alpha$  concentrations were determined by single-molecule array (Simoa) on a HD-1 Analyzer (Quanterix) using a commercial kit for IFN- $\alpha$ 2 quantification (Quanterix). Whole blood was collected on PAXgene blood RNA tubes (BD Biosciences) or on EDTA tubes for IFN signature, RNA extraction was performed with the kit maxwell 16 LEV simply RNA blood associated with the Maxwell extractor (Promega) and quantified by absorbance (Nanovue). IFN score was obtained using nCounter analysis technology (NanoString Technologies) by calculating the median of the normalized count of 6 ISGs as previously described(44)

### T-cell V $\beta$ repertoire analysis and immunophenotyping

The phenotypic analysis of T-cell V $\beta$  repertoire was performed on whole blood sample using the IOTest Beta Mark kit (Beckman-Coulter) containing 24 monoclonal antibodies (mAbs) identifying ~ 70% of the T cell repertoire. Whole blood cells were stained with APC-Alexa Fluor 750-conjugated anti-CD3, Pacific Blue-conjugated anti-CD4, Krome Orange-conjugated anti-CD8 and each combination of 3 FITC-, PE- and FITC/PE-conjugated anti-V $\beta$  mAbs (Beckman-Coulter) in 8 sample tubes. Whole blood sample were lysed with OptiLyse C Lysing Solution (Beckman-Coulter), washed and fixed in 0.5% formaldehyde in PBS.  $0.5$  to  $10^4$  T cells were acquired on a NAVIOS flow cytometer and data were analyzed using NAVIOS software. Lymphocytes were first gated according to FSC/SSC parameter, then by selection of CD3+, CD4+ and CD3+CD4- positive cells. The proportion of each V $\beta$  family was compared to the minimum and the mean+2SD of each reference values obtained from data from IOTest Beta Mark® kit to evaluate expanded or restricted V $\beta$  family. Expansions or restrictions were defined respectively for values above the mean+2SD or below the minimum reference values of the corresponding family.

### Lymphocytes immunophenotyping

CD3, CD4 and CD8 T lymphocyte subsets were enumerated on EDTA-anticoagulated peripheral whole blood by single-platform the fully automated volumetric single platform technology flow cytometer AQUIOS CL (Beckman-Coulter) as previously described(45). The phenotypic characterization of B, NK and T activated lymphocyte subsets were performed on EDTA-anticoagulated whole blood using the following combination of monoclonal antibodies: APC-Alexa Fluor 750-conjugated anti-CD3, Pacific Blue-conjugated anti-CD4, Krome Orange-conjugated anti-CD8, FITC-conjugated anti-HLA-DR, APC-conjugated anti-CD19, Krome Orange-conjugated anti-CD16 and ECD-conjugated anti-CD56 (Beckman-Coulter). The preparations were lysed and fixed by thoroughly mixing and incubating for 10 min successively with 500 $\mu\text{L}$  of OptiLyse C reagent (Beckman-Coulter) and 1mL of PBS. The cells were centrifuged for 5min at 400g, resuspended in 500 $\mu\text{L}$  of PBS and acquired on a NAVIOS flow cytometer (Beckman-Coulter).

### Nanostring TCR expression analysis

Total RNA was extracted from PAXgene™ tubes using the Maxwell® 16 LEV simplyRNA Blood kit (Promega), following the manufacturer's guidelines. The RNA quantity was determined using a Nanodrop (Thermo Scientific). 200 ng total RNA were hybridized with the nCounter® T cell repertoire panel (Nanostring®, #LBL-10805-01) and counted on an nCounter® FLEX platform according to the manufacturer's guidelines. Raw counts were normalized using internal positive standards and 12 housekeeping genes. Raw counts of *TRBV* genes were expressed as a proportion among total *TRBV* gene counts for each patient and normalized using the median value from the healthy control group.

### Monocyte HLA-DR expression assessment

Monocyte HLA-DR expression was determined on EDTA-anticoagulated peripheral whole blood as previously described(46).

### TCR-sequencing

RNA was extracted from whole blood as reported above. T cell receptor (TCR) alpha/beta libraries were prepared from 300ng of RNA from each sample with SMARTer Human TCR a/b Profiling Kit (Takarabio) following provider protocol as previously described (32). Briefly, the reverse transcription was performed using a mixture of TRBC and TRAC reverse primers and further extended with a template-switching oligonucleotide (SMART-Seq v4). cDNAs were then amplified following two semi-nested PCR: a first PCR with TRBC and TRAC reverse primers as well as a forward primer hybridizing to the SMART-Seq v4 sequence added by template-switching and a second PCR targeting the PCR1 amplicons with reverse and forward primer including Illumina Indexes allowing for sample barcoding. PCR2 are then purified using AMPure XP beads (Beckman-Coulter). The sequencing was then carried out on a MiSeq Illumina sequencer using the MiSeq v3 PE300 protocol at the Biomics Platform (Institut Pasteur, Paris, France). Single end sequences were aligned and annotated using MiXCR 3.0.13 (47), providing a list of clonotypes, each of which is defined as a unique combination of one *TRBV* gene with one CDR3 amino-acid sequence and one *TRBJ* gene.

### TCR-Seq repertoire analysis

Analyses were performed in R 4.0.3 on the TRB clonotype lists obtained with MiXCR. For each clonotype, read count was recorded. Frequencies for *TRBV*, *TRBJ* and clonotypes were calculated based on the total read counts per sample. Chord diagrams were made using the circlize package(48) on *TRBVBJ* frequencies, CDR3 length spectratypes were made using ggplot2 (49) using clonotype frequencies. To identify *TRBV11-2* expanded clonotypes, first (Q1) and third (Q3) quartiles and the interquartile range (IQR) were computed for all patients without *TRBV11-2* expansion. Expanded clonotypes are defined as those with counts superiors to  $Q3+(1.5*IQR)$ .

### Immunophenotyping of Vβ 21.3+ T cells

Thawed PBMC were labeled using Fixable Viability Dye eFluor™ 506 from Thermo Fisher. PBMCs were stained with surface markers, APC-conjugated anti-

CD3, BUV486- conjugated anti-CD4, PE-Cy7-conjugated anti-CD8, APC-Cy7-conjugated anti-CD14, APC-Cy7-conjugated anti-CD16, APC-Cy7-conjugated anti-CD19, BV711-conjugated anti-CCR7 and BV421-conjugated anti-CD38 (BioLegend), FITC-conjugated anti-Vb21.3 (Miltenyi), Biotin-conjugated anti-HLA-DR, APC-conjugated CX3CR1 (Ebiosciences), BV605-conjugated anti-CD45RA and streptavidine-conjugated PE-texas Red (BD). Cells were then washed, fixed with PBS/Formalin 2% (Sigma-Aldrich). Cell apoptosis was assessed by annexin V staining with the PE Annexin V Apoptosis Detection Kit I (BD). All samples were acquired on a BD LSRFortessa (BD Biosciences) flow cytometer and analyzed using FlowJo version 10 software.

### **Stimulation with SARS-CoV-2 overlapping peptide pools and flow cytometry**

Briefly, overnight-rested PBMCs were stimulated with SARS-CoV-2 PepTivator pooled peptides (Miltenyi Biotec) at a final concentration of 2  $\mu\text{g ml}^{-1}$  for 1 h in the presence of 2  $\mu\text{g ml}^{-1}$  monoclonal antibodies CD28 and CD49d, and then for an additional 5 h with GolgiPlug and GolgiStop (BD Biosciences). Dead cells were labeled using LIVE/DEAD Fixable near IR dye from Invitrogen. Surface markers, including APC-conjugated anti-CD3, BUV486- conjugated anti-CD4, PE-Cy7-conjugated anti-CD8, APC-Cy7-conjugated anti-CD14, APC-Cy7-conjugated anti-CD16 and APC-Cy7-conjugated anti-CD19 (BioLegend) and FITC-conjugated anti-Vb21.3 (Miltenyi) were stained. Cells were then washed, fixed with Cytfix/Cytoperm (BD Biosciences) and stained with V450- conjugated anti-IFN $\gamma$  (eBioscience). Negative controls without peptide stimulation were run for each sample. All samples were acquired on a BD LSRFortessa (BD Biosciences) flow cytometer and analyzed using FlowJo version 10 software.

### **Serology**

Serum samples were tested with three commercial assays: the Wantai Ab assay detecting total antibodies against the receptor binding domain (RBD) of the S protein, the bioMérieux Vidas assay detecting IgG to the RBD and the Abbott Architect assay detecting IgG to the N protein.

### **Statistical analyses**

PCA analysis was made in R with stats package and visualized with ggplot2 (49) for Vbeta frequencies obtained by flow cytometry. All statistical analyses were performed using GraphPad with the help of a trained biostatistician.

### **Supplementary Material**

Refer to Web version on PubMed Central for supplementary material.

### **Acknowledgments:**

We thank the patients and families that contributed to this work. We also thank L. Ma, and L. Lemée from the Biomics Platform C2RT, Institut Pasteur (Paris, France), supported by France Génomique (ANR-10-INBS-09-09) and IBISA. Human biological samples and associated data were obtained from NeuroBioTec (CRB HCL, Lyon France, Biobank BB-0033-00046). We acknowledge Guy Oriol for technical advices.

**Fundings:**

This work was supported by Fondation Hospices Civils de Lyon, Square Foundation, Grandir – Fonds de solidarité pour l'enfance and Olympique Lyonnais Foundation. KLG work is supported by the AIR-MI grant (ANR-18-ECVD-0001). EMF is funded by AIR-MI (ANR-18-ECVD-0001) and iReceptorPlus (H2020 Research and Innovation Programme 825821) grants. DK contributions are funded by iMAP (ANR-16-RHUS-0001), Transimmunom LabEX (ANR-11-IDEX-0004-02), TriPoD ERC Research Advanced Grant (Fp7-IdEAS-ErC-322856).

**References**

1. Riphagen S, Gomez X, Gonzalez-Martinez C, Wilkinson N, Theocharis P, Hyperinflammatory shock in children during COVID-19 pandemic. *The Lancet*. 395, 1607–1608 (2020).
2. Verdoni L, Mazza A, Gervasoni A, Martelli L, Ruggeri M, Ciuffreda M, Bonanomi E, D'Antiga L, An outbreak of severe Kawasaki-like disease at the Italian epicentre of the SARS-CoV-2 epidemic: an observational cohort study. *The Lancet*. 0 (2020), doi:10.1016/S0140-6736(20)31103-X.
3. Belot A, Antona D, Renolleau S, Javouhey E, Hentgen V, Angoulvant F, Delacourt C, Iriart X, Ovaert C, Bader-Meunier B, Kone-Paut I, Levy-Bruhl D, SARS-CoV-2-related paediatric inflammatory multisystem syndrome, an epidemiological study, France, 1 March to 17 May 2020. *Eurosurveillance*. 25, 2001010 (2020).
4. Levin M, Childhood Multisystem Inflammatory Syndrome - A New Challenge in the Pandemic. *N. Engl. J. Med* (2020), doi:10.1056/NEJMe2023158.
5. Dufort EM, Koumans EH, Chow EJ, Rosenthal EM, Muse A, Rowlands J, Barranco MA, Maxted AM, Rosenberg ES, Easton D, Udo T, Kumar J, Pulver W, Smith L, Hutton B, Blog D, Zucker H, New York State and Centers for Disease Control and Prevention Multisystem Inflammatory Syndrome in Children Investigation Team, Multisystem Inflammatory Syndrome in Children in New York State. *N. Engl. J. Med* (2020), doi:10.1056/NEJMoa2021756.
6. Feldstein LR, Rose EB, Horwitz SM, Collins JP, Newhams MM, Son MBF, Newburger JW, Kleinman LC, Heidemann SM, Martin AA, Singh AR, Li S, Tarquinio KM, Jaggi P, Oster ME, Zackai SP, Gillen J, Ratner AJ, Walsh RF, Fitzgerald JC, Keenaghan MA, Alharash H, Doymaz S, Clouser KN, Giuliano JS, Gupta A, Parker RM, Maddux AB, Havalad V, Ramsingh S, Bukulmez H, Bradford TT, Smith LS, Tenforde MW, Carroll CL, Riggs BJ, Gertz SJ, Daube A, Lansell A, Coronado Munoz A, Hobbs CV, Marohn KL, Halasa NB, Patel MM, Randolph AG, Multisystem Inflammatory Syndrome in U.S. Children and Adolescents. *N. Engl. J. Med* (2020), doi:10.1056/NEJMoa2021680.
7. Belot A, Levy-Bruhl D, French Covid-19 Pediatric Inflammation Consortium, Multisystem Inflammatory Syndrome in Children in the United States. *N Engl J Med*. 383, 1793–1794 (2020). [PubMed: 33085852]
8. Consiglio CR, Cotugno N, Sardh F, Pou C, Amodio D, Rodriguez L, Tan Z, Zicari S, Ruggiero A, Pascucci GR, Santilli V, Campbell T, Bryceson Y, Eriksson D, Wang J, Marchesi A, Lakshmikanth T, Campana A, Villani A, Rossi P, CACTUS Study Team, Landegren N, Palma P, Brodin P, The Immunology of Multisystem Inflammatory Syndrome in Children with COVID-19. *Cell*. 183, 968–981.e7 (2020). [PubMed: 32966765]
9. Diorio C, Henrickson SE, Vella LA, McNerney KO, Chase J, Burudpakdee C, Lee JH, Jasen C, Balamuth F, Barrett DM, Banwell BL, Bernt KM, Blatz AM, Chiotos K, Fisher BT, Fitzgerald JC, Gerber JS, Gollomp K, Gray C, Grupp SA, Harris RM, Kilbaugh TJ, John ARO, Lambert M, Liebling EJ, Paessler ME, Petrosa W, Phillips C, Reilly AF, Romberg ND, Seif A, Sesok-Pizzini DA, Sullivan KE, Vardaro J, Behrens EM, Teachey DT, Bassiri H, Multisystem inflammatory syndrome in children and COVID-19 are distinct presentations of SARS-CoV-2. *J Clin Invest*. 130, 5967–5975 (2020). [PubMed: 32730233]
10. Carter MJ, Fish M, Jennings A, Doores KJ, Wellman P, Seow J, Acors S, Graham C, Timms E, Kenny J, Neil S, Malim MH, Tibby SM, Shankar-Hari M, Peripheral immunophenotypes in children with multisystem inflammatory syndrome associated with SARS-COV-2 infection. *Nat Med* (2020), doi:10.1038/s41591-020-1054-6.
11. Gruber CN, Patel RS, Trachtman R, Lepow L, Amanat F, Krammer F, Wilson KM, Onel K, Geanon D, Tuballes K, Patel M, Mouskas K, O'Donnell T, Merritt E, Simons NW, Barcessat V,

- Del Valle DM, Udondem S, Kang G, Gangadharan S, Ofori-Amanfo G, Laserson U, Rahman A, Kim-Schulze S, Charney AW, Gnjatich S, Gelb BD, Merad M, Bogunovic D, Mapping Systemic Inflammation and Antibody Responses in Multisystem Inflammatory Syndrome in Children (MIS-C). *Cell*. 183, 982–995.e14 (2020). [PubMed: 32991843]
12. Schwartz A, Belot A, Kone-Paut I, Pediatric Inflammatory Multisystem Syndrome and Rheumatic Diseases During SARS-CoV-2 Pandemic. *Front. Pediatr* 8 (2020), doi:10.3389/fped.2020.605807.
  13. Casanova J-L, Su HC, A global effort to define the human genetics of protective immunity to SARS-CoV-2 infection. *Cell*. 0 (2020), doi:10.1016/j.cell.2020.05.016.
  14. Sancho-Shimizu V, Brodin P, Cobat A, Biggs CM, Toubiana J, Lucas CL, Henrickson SE, Belot A, MIS-C@CHGE, Tangye SG, Milner JD, Levin M, Abel L, Bogunovic D, Casanova J-L, Zhang S-Y, SARS-CoV-2–related MIS-C: A key to the viral and genetic causes of Kawasaki disease? *Journal of Experimental Medicine*. 218 (2021), doi:10.1084/jem.20210446.
  15. Trouillet-Assant S, Viel S, Gaymard A, Pons S, Richard J, Perret M, Villard M, Brengel-Pesce K, Lina B, Mezidi M, Bitker L, Belot A, Type I IFN immunoprofiling in COVID-19 patients. *J Allergy Clin Immunol*. 146, 206–208.e2 (2020). [PubMed: 32360285]
  16. Hadjadj J, Yatim N, Barnabei L, Corneau A, Boussier J, Smith N, Péré H, Charbit B, Bondet V, Chenevier-Gobeaux C, Breillat P, Carlier N, Gauzit R, Morbieu C, Pène F, Marin N, Roche N, Szwebel T-A, Merklings SH, Treluyer J-M, Veyer D, Mouthon L, Blanc C, Tharaux P-L, Rozenberg F, Fischer A, Duffy D, Rieux-Laucat F, Kernéis S, Terrier B, Impaired type I interferon activity and inflammatory responses in severe COVID-19 patients. *Science* (2020), doi:10.1126/science.abc6027.
  17. Bastard P, Rosen LB, Zhang Q, Michailidis E, Hoffmann H-H, Zhang Y, Dorgham K, Philippot Q, Rosain J, Béziat V, Manry J, Shaw E, Haljasmägi L, Peterson P, Lorenzo L, Bizien L, Trouillet-Assant S, Dobbs K, de Jesus AA, Belot A, Kallaste A, Catherinot E, Tandjaoui-Lambiotte Y, Le Pen J, Kerner G, Bigio B, Seeleuthner Y, Yang R, Bolze A, Spaan AN, Delmonte OM, Abers MS, Aiuti A, Casari G, Lampasona V, Piemonti L, Ciceri F, Bilguvar K, Lifton RP, Vasse M, Smadja DM, Migaud M, Hadjadj J, Terrier B, Duffy D, Quintana-Murci L, van de Beek D, Roussel L, Vinh DC, Tangye SG, Haerynck F, Dalmau D, Martinez-Picado J, Brodin P, Nussenzweig MC, Boisson-Dupuis S, Rodríguez-Gallego C, Vogt G, Mogensen TH, Oler AJ, Gu J, Burbelo PD, Cohen JI, Biondi A, Bettini LR, D’Angio M, Bonfanti P, Rossignol P, Mayaux J, Rieux-Laucat F, Husebye ES, Fusco F, Ursini MV, Imberti L, Sottini A, Paghera S, Quiros-Roldan E, Rossi C, Castagnoli R, Montagna D, Licari A, Marseglia GL, Duval X, Ghosn J, HGID Lab, NIAID-USUHS Immune Response to COVID Group, COVID Clinicians, COVID-STORM Clinicians, Imagine COVID Group, French COVID Cohort Study Group, Milieu Interieur Consortium, CoV-Contact Cohort, Amsterdam UMC Covid-19 Biobank, COVID Human Genetic Effort, Tsang JS, Goldbach-Mansky R, Kisand K, Lionakis MS, Puel A, Zhang S-Y, Holland SM, Gorochov G, Jouanguy E, Rice CM, Cobat A, Notarangelo LD, Abel L, Su HC, Casanova J-L, Autoantibodies against type I IFNs in patients with life-threatening COVID-19. *Science*. 370 (2020), doi:10.1126/science.abd4585.
  18. Zhang Q, Bastard P, Liu Z, Le Pen J, Moncada-Velez M, Chen J, Ogishi M, Sabli IKD, Hodeib S, Korol C, Rosain J, Bilguvar K, Ye J, Bolze A, Bigio B, Yang R, Arias AA, Zhou Q, Zhang Y, Onodi F, Korniotis S, Karpf L, Philippot Q, Chbihi M, Bonnet-Madin L, Dorgham K, Smith N, Schneider WM, Razoogy BS, Hoffmann H-H, Michailidis E, Moens L, Han JE, Lorenzo L, Bizien L, Meade P, Neehus A-L, Ugurbil AC, Corneau A, Kerner G, Zhang P, Rapaport F, Seeleuthner Y, Manry J, Masson C, Schmitt Y, Schlüter A, Le Voyer T, Khan T, Li J, Fellay J, Roussel L, Shahrooei M, Alosaimi MF, Mansouri D, Al-Saud H, Al-Mulla F, Almourfi F, Al-Muhsen SZ, Alshime F, Al Turki S, Hasanato R, van de Beek D, Biondi A, Bettini LR, D’Angio M, Bonfanti P, Imberti L, Sottini A, Paghera S, Quiros-Roldan E, Rossi C, Oler AJ, Tompkins MF, Alba C, Vandernoot I, Goffard J-C, Smits G, Migeotte I, Haerynck F, Soler-Palacin P, Martin-Nalda A, Colobran R, Morange P-E, Keles S, Çölkesen F, Ozelik T, Yasar KK, Senoglu S, Karabela N, Rodríguez-Gallego C, Novelli G, Hraiech S, Tandjaoui-Lambiotte Y, Duval X, Laouénan C, COVID-STORM Clinicians, COVID Clinicians, Imagine COVID Group, French COVID Cohort Study Group, CoV-Contact Cohort, Amsterdam UMC Covid-19 Biobank, COVID Human Genetic Effort, NIAID-USUHS/TAGC COVID Immunity Group, Snow AL, Dalgard CL, Milner JD, Vinh DC, Mogensen TH, Marr N, Spaan AN, Boisson B, Boisson-Dupuis S, Bustamante J, Puel A, Ciancanelli MJ, Meyts I, Maniatis T, Soumelis V, Amara A, Nussenzweig M, García-Sastre A,



- Krammer F, Pujol A, Duffy D, Lifton RP, Zhang S-Y, Gorochov G, Béziat V, Jouanguy E, Sancho-Shimizu V, Rice CM, Abel L, Notarangelo LD, Cobat A, Su HC, Casanova J-L. Inborn errors of type I IFN immunity in patients with life-threatening COVID-19. *Science*. 370 (2020), doi:10.1126/science.abd4570.
19. Choi Y, Lafferty JA, Clements JR, Todd JK, Gelfand EW, Kappler J, Marrack P, Kotzin BL, Selective expansion of T cells expressing V beta 2 in toxic shock syndrome. *J Exp Med*. 172, 981–984 (1990). [PubMed: 2117641]
  20. Thomas D, Dauwalder O, Brun V, Badiou C, Ferry T, Etienne J, Vandenesch F, Lina G, *Staphylococcus aureus* superantigens elicit redundant and extensive human Vbeta patterns. *Infect Immun*. 77, 2043–2050 (2009). [PubMed: 19255190]
  21. Collette A, Six A, ISEApeaks: an Excel platform for GeneScan and Immunoscope data retrieval, management and analysis. *Bioinformatics*. 18, 329–330 (2002). [PubMed: 11847085]
  22. Vella LA, Giles JR, Baxter AE, Oldridge DA, Diorio C, Kuri-Cervantes L, Alanio C, Pampena MB, Wu JE, Chen Z, Huang YJ, Anderson EM, Gouma S, McNERney KO, Chase J, Burudpakdee C, Lee JH, Apostolidis SA, Huang AC, Mathew D, Kuthuru O, Goodwin EC, Weirick ME, Bolton MJ, Arevalo CP, Ramos A, Jasen CJ, Conrey PE, Sayed S, Giannini HM, D’Andrea K, UPenn COVID Processing Unit, Meyer NJ, Behrens EM, Bassiri H, Hensley SE, Henrickson SE, Teachey DT, Betts MR, Wherry EJ, Deep immune profiling of MIS-C demonstrates marked but transient immune activation compared to adult and pediatric COVID-19. *Sci Immunol*. 6 (2021), doi:10.1126/sciimmunol.abf7570.
  23. Ouldali N, Toubiana J, Antona D, Javouhey E, Madhi F, Lorrot M, Leger P-L, Galeotti C, Claude C, Wiedemann A, Lachaume N, Ovaert C, Dumortier M, Kahn J-E, Mandelewajg A, Percheron L, Biot B, Bordet J, Girardin M-L, Yang DD, Grimaud M, Oualha M, Allali S, Bajolle F, Beyler C, Meinzer U, Levy M, Paulet A-M, Levy C, Cohen R, Belot A, Angoulvant F, French Covid-19 Paediatric Inflammation Consortium, Association of Intravenous Immunoglobulins Plus Methylprednisolone vs Immunoglobulins Alone With Course of Fever in Multisystem Inflammatory Syndrome in Children. *JAMA* (2021), doi:10.1001/jama.2021.0694.
  24. Todd JK, Ressler M, Caston SA, Todd BH, Wiesenthal AM, Corticosteroid therapy for patients with toxic shock syndrome. *JAMA*. 252, 3399–3402 (1984). [PubMed: 6389917]
  25. Leung DY, Meissner C, Fulton D, Schlievert PM, The potential role of bacterial superantigens in the pathogenesis of Kawasaki syndrome. *J Clin Immunol*. 15, 11S–17S (1995). [PubMed: 8613483]
  26. Esper F, Shapiro ED, Weibel C, Ferguson D, Landry ML, Kahn JS, Association between a Novel Human Coronavirus and Kawasaki Disease. *J Infect Dis*. 191, 499–502 (2005). [PubMed: 15655771]
  27. Esteve-Sole A, Anton J, Pino-Ramirez RM, Sanchez-Manubens J, Fumadó V, Fortuny C, Rios-Barnes M, Sanchez-de-Toledo J, Girona-Alarcón M, Mosquera JM, Ricart S, Launes C, de Sevilla MF, Jou C, Muñoz-Almagro C, González-Roca E, Vergara A, Carrillo J, Juan M, Cuadras D, Noguera-Julian A, Jordan I, Alsina L, Similarities and differences between the immunopathogenesis of COVID-19-related pediatric multisystem inflammatory syndrome and Kawasaki disease. *J Clin Invest*. 131 (2021), doi:10.1172/JCI144554.
  28. Lee PY, Platt CD, Weeks S, Grace RF, Maher G, Gauthier K, Devana S, Vitali S, Randolph AG, McDonald DR, Geha RS, Chou J, Immune dysregulation and multisystem inflammatory syndrome in children (MIS-C) in individuals with haploinsufficiency of SOCS1. *J Allergy Clin Immunol* (2020), doi:10.1016/j.jaci.2020.07.033.
  29. Hadjadj J, Castro CN, Tusseau M, Stolzenberg M-C, Mazerolles F, Aladjidi N, Armstrong M, Ashrafiyan H, Cutcutache I, Ebetsberger-Dachs G, Elliott KS, Durieu I, Fabien N, Fusaro M, Heeg M, Schmitt Y, Bras M, Knight JC, Lega J-C, Lesca G, Mathieu A-L, Moreews M, Moreira B, Nosbaum A, Page M, Picard C, Ronan Leahy T, Rouvet I, Ryan E, Sanlaville D, Schwarz K, Skelton A, Viillard J-F, Viel S, Viillard M, Callebaut I, Picard C, Walzer T, Ehl S, Fischer A, Neven B, Belot A, Rieux-Laucat F, Early-onset autoimmunity associated with SOCS1 haploinsufficiency. *Nat Commun*. 11, 5341 (2020). [PubMed: 33087723]
  30. Remy S, Gossez M, Belot A, Hayman J, Portefaix A, Venet F, Javouhey E, Monneret G, Massive increase in monocyte HLA-DR expression can be used to discriminate between septic shock

- and hemophagocytic lymphohistiocytosis-induced shock. *Crit Care*. 22, 213 (2018). [PubMed: 30205835]
31. Monneret G, Elmenkouri N, Bohe J, Debard A-L, Gutowski M-C, Bienvenu J, Lepape A, Analytical requirements for measuring monocytic human lymphocyte antigen DR by flow cytometry: application to the monitoring of patients with septic shock. *Clin Chem*. 48, 1589–1592 (2002). [PubMed: 12194941]
  32. The V $\beta$ -specific superantigen staphylococcal enterotoxin B: Stimulation of mature T cells and clonal deletion in neonatal mice. *Cell*. 56, 27–35 (1989). [PubMed: 2521300]
  33. Venet F, Lukaszewicz A-C, Payen D, Hotchkiss R, Monneret G, Monitoring the immune response in sepsis: a rational approach to administration of immunoadjuvant therapies. *Curr Opin Immunol*. 25, 477–483 (2013). [PubMed: 23725873]
  34. Porritt RA, Paschold L, Rivas MN, Cheng MH, Yonker LM, Chandnani H, Lopez M, Simnica D, Schultheiß C, Santiskulvong C, Van Eyk J, Fasano A, Bahar I, Binder M, Arditì M, Identification of a unique TCR repertoire, consistent with a superantigen selection process in Children with Multi-system Inflammatory Syndrome. *bioRxiv* (2020), doi:10.1101/2020.11.09.372169.
  35. Ramaswamy A, Brodsky NN, Sumida TS, Comi M, Asashima H, Hoehn KB, Li N, Liu Y, Shah A, Ravindra NG, Bishai J, Khan A, Lau W, Sellers B, Bansal N, Sparks R, Unterman A, Habet V, Rice AJ, Catanzaro J, Chandnani H, Lopez M, Kaminski N, Dela Cruz CS, Tsang JS, Wang Z, Yan X, Kleinstein SH, van Dijk D, Pierce RW, Hafler DA, Lucas CL, Post-infectious inflammatory disease in MIS-C features elevated cytotoxicity signatures and autoreactivity that correlates with severity. *medRxiv* (2020), doi:10.1101/2020.12.01.20241364.
  36. Porritt RA, Paschold L, Noval Rivas M, Cheng MH, Yonker LM, Chandnani H, Lopez M, Simnica D, Schultheiß C, Santiskulvong C, van Eyk J, McCormick JK, Fasano A, Bahar I, Binder M, Arditì M, HLA class I-associated expansion of TRBV11-2 T cells in Multisystem Inflammatory Syndrome in Children. *J Clin Invest* (2021), doi:10.1172/JCI146614.
  37. Tanaka Y, Hoshino-Negishi K, Kuboi Y, Tago F, Yasuda N, Imai T, Emerging Role of Fractalkine in the Treatment of Rheumatic Diseases. *Immunotargets Ther*. 9, 241–253 (2020). [PubMed: 33178636]
  38. Ramaswamy A, Brodsky NN, Sumida TS, Comi M, Asashima H, Hoehn KB, Li N, Liu Y, Shah A, Ravindra NG, Bishai J, Khan A, Lau W, Sellers B, Bansal N, Guerrero P, Unterman A, Habet V, Rice AJ, Catanzaro J, Chandnani H, Lopez M, Kaminski N, Dela Cruz CS, Tsang JS, Wang Z, Yan X, Kleinstein SH, van Dijk D, Pierce RW, Hafler DA, Lucas CL, Immune dysregulation and autoreactivity correlate with disease severity in SARS-CoV-2-associated multisystem inflammatory syndrome in children. *Immunity* (2021), doi:10.1016/j.immuni.2021.04.003.
  39. Kappler J, Kotzin B, Herron L, Gelfand EW, Bigler RD, Boylston A, Carrel S, Posnett DN, Choi Y, Marrack P, V beta-specific stimulation of human T cells by staphylococcal toxins. *Science*. 244, 811–813 (1989). [PubMed: 2524876]
  40. Hoffman M, “Superantigens” may shed light on immune puzzle. *Science*. 248, 685–686 (1990). [PubMed: 2333520]
  41. Cheng MH, Zhang S, Porritt RA, Noval Rivas M, Paschold L, Willscher E, Binder M, Arditì M, Bahar I, Superantigenic character of an insert unique to SARS-CoV-2 spike supported by skewed TCR repertoire in patients with hyperinflammation. *Proc Natl Acad Sci U S A*. 117, 25254–25262 (2020). [PubMed: 32989130]
  42. Brogan PA, Shah V, Klein N, Dillon MJ, Vbeta-restricted T cell adherence to endothelial cells: a mechanism for superantigen-dependent vascular injury. *Arthritis Rheum*. 50, 589–597 (2004). [PubMed: 14872503]
  43. Bartsch YC, Wang C, Zohar T, Fischinger S, Atyeo C, Burke JS, Kang J, Edlow AG, Fasano A, Baden LR, Nilles EJ, Woolley AE, Karlson EW, Hopke AR, Irimia D, Fischer ES, Ryan ET, Charles RC, Julg BD, Lauffenburger DA, Yonker LM, Alter G, Humoral signatures of protective and pathological SARS-CoV-2 infection in children. *Nat Med*. 27, 454–462 (2021). [PubMed: 33589825]
  44. Pescarmona R, Belot A, Villard M, Besson L, Lopez J, Mosnier I, Mathieu A-L, Lombard C, Garnier L, Frachette C, Walzer T, Viel S, Comparison of RT-qPCR and Nanostring in the

- measurement of blood interferon response for the diagnosis of type I interferonopathies. *Cytokine*. 113, 446–452 (2019). [PubMed: 30413290]
45. Gossez M, Malcus C, Demaret J, Frater J, Poitevin-Later F, Monneret G, Evaluation of a novel automated volumetric flow cytometer for absolute CD4+ T lymphocyte quantitation. *Cytometry B Clin Cytom.* 92, 456–464 (2017). [PubMed: 26804473]
  46. Demaret J, Walencik A, Jacob M-C, Timsit J-F, Venet F, Lepape A, Monneret G, Inter-laboratory assessment of flow cytometric monocyte HLA-DR expression in clinical samples. *Cytometry B Clin Cytom.* 84, 59–62 (2013). [PubMed: 22987669]
  47. Bolotin DA, Poslavsky S, Mitrophanov I, Shugay M, Mamedov IZ, Putintseva EV, Chudakov DM, MiXCR: software for comprehensive adaptive immunity profiling. *Nature Methods.* 12, 380–381 (2015). [PubMed: 25924071]
  48. Gu Z, Gu L, Eils R, Schlesner M, Brors B, circlize implements and enhances circular visualization in R. *Bioinformatics.* 30, 2811–2812 (2014). [PubMed: 24930139]
  49. Wickham H, *Ggplot2: elegant graphics for data analysis* (Springer, New York, 2009), Use R!
  50. Rice GI, Forte G, Szykiewicz M, Chase DS, Aeby A, Abdel-Hamid MS, Ackroyd S, Allcock R, Bailey KM, Balottin U, Assessment of interferon-related biomarkers in Aicardi-Goutières syndrome associated with mutations in *TREX1*, *RNASEH2A*, *RNASEH2B*, *RNASEH2C*, *SAMHD1*, and *ADAR*: a case-control study. *The Lancet Neurology.* 12, 1159–1169 (2013). [PubMed: 24183309]

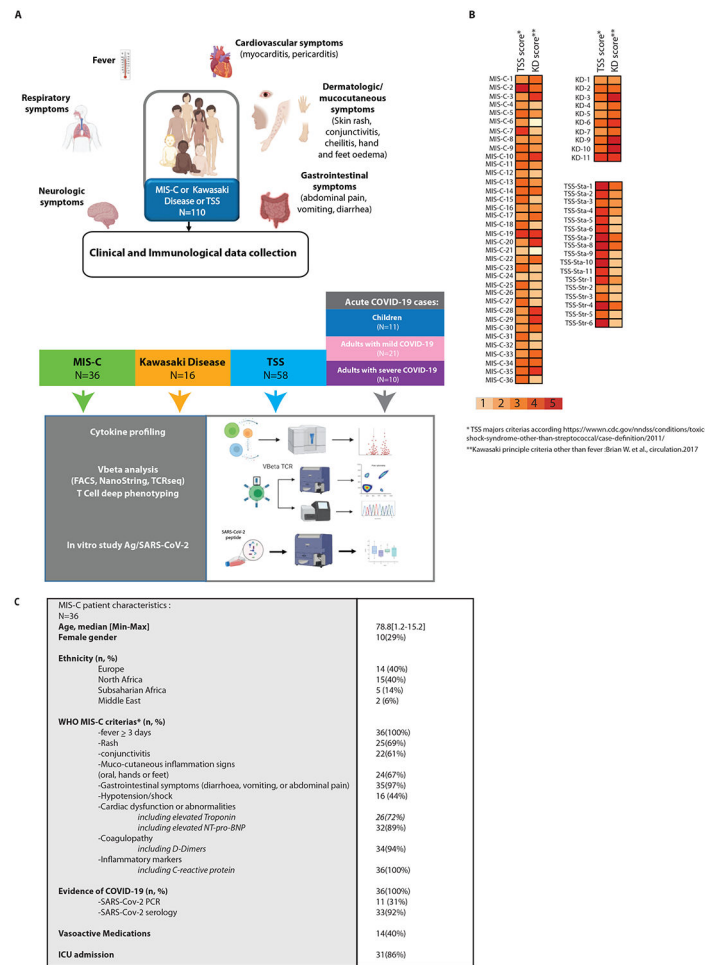


**Figure 1. Study design and clinical features of MIS-C patients**  
 (A) Outline of the study including MIS-C, KD, TSS and acute COVID-19 patients and the immunological investigation workflow. (B) Heatmap showing the TSS or KD clinical score for TSS, MIS-C and KD patients included in our study, calculated as the number of major criteria reached for each disease. (C) Clinical description of all MIS-C patients included in the study.

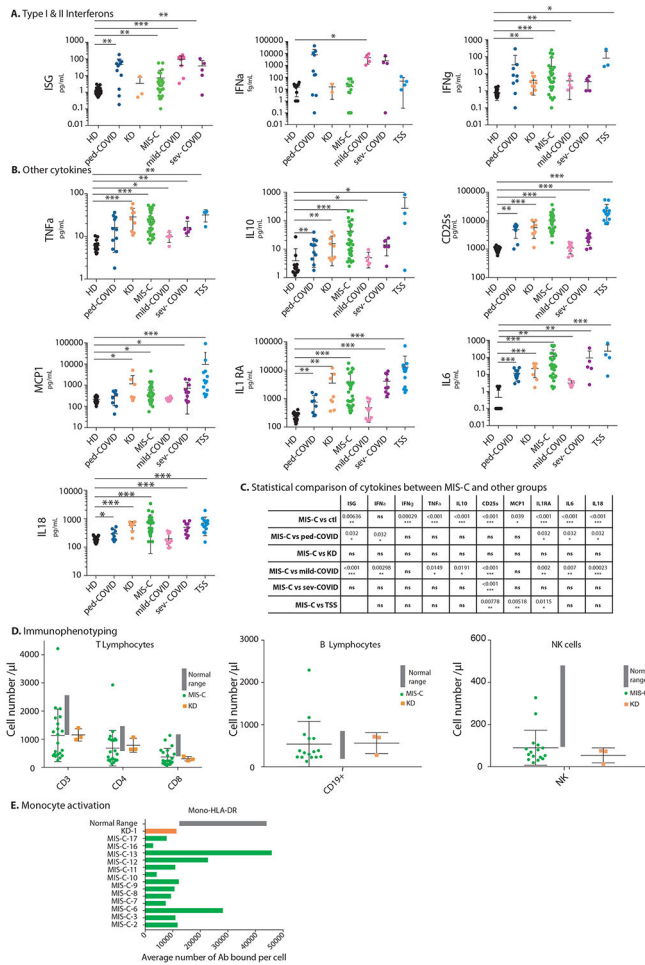


**Figure 2. Systemic inflammation and signs of immune paralysis in MIS-C patients** (A) Left panel: Interferon score calculated as the normalized mean expression of six ISGs measured using the Nanostring technology, as previously described (44, 50). Middle panel: Serum IFN- $\alpha$ , in different groups of patients, as measured with the Simoa technology. Right panel: Serum IFN- $\gamma$  level measured by Elisa. N=3 to 30 per group, as indicated in Table S2; Statistical test: multiple comparisons and correction using Benjamini-Hochberg procedure. (B). Serum levels of the indicated cytokines as measured by automated ELISA. N=5 to 30 per group, as indicated in Table S2; Statistical test: multiple comparisons and correction using Benjamini-Hochberg procedure. (C) Table showing the statistical results of the comparison of cytokine levels between MIS-C and other groups, as indicated. (D) T, B and NK lymphocyte counts measured by flow cytometry in MIS-C and KD. The grey bar indicates the normal range in healthy donors . N=3 to 13 per group, as indicated in Table S2. (E) HLA-DR expression in T cells and monocytes, as measured by flow cytometry in MIS-C. The grey bar indicates the normal range in healthy donors. \*P < 0.05, \*\*P < 0.01, \*\*\*P < 0.001.

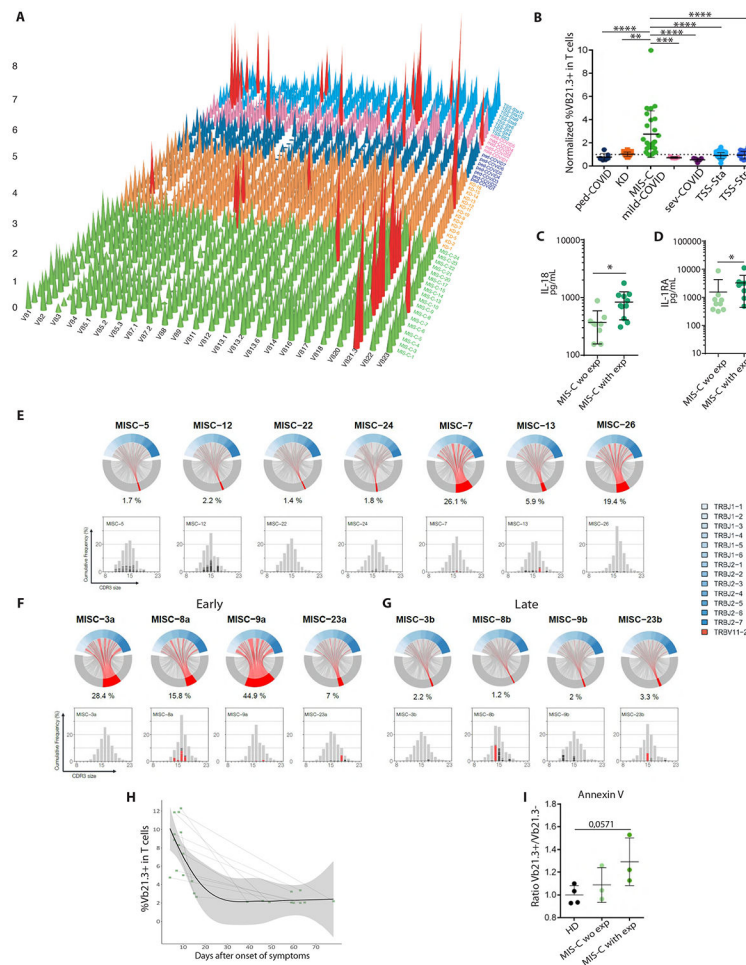


**Figure 3. Polyclonal Vb21.3+ T cell expansion in MIS-C patients**

(A) Frequency of total CD3<sup>+</sup> T cells expressing the indicated Vβ chains, as measured by flow cytometry using specific antibodies against the corresponding Vβ within PBMCs of patients of the indicated group. TSS, mild COVID-19, pediatric COVID-19 (ped-COVID), KD and MIS-C patients are colored in blue, pink, dark blue, orange and green respectively. The red color highlights values at least twice higher as the mean frequency in the general adult population. (B) Normalized frequency of Vβ21.3<sup>+</sup> T cells in different clinical conditions, as indicated. N=5 to 26 per group, as indicated in Table S2; Statistical test: Mann-Whitney using FDR adjustment. (C-D) Serum IL-18 (C) and IL-1RA (D) levels in MIS-C patients with or without Vβ21.3<sup>+</sup> T cell expansions (exp). N=6 to 11 per group, as indicated in Table S2; Statistical test: Mann-Whitney. (E-G) Chord diagrams of the TRBV (bottom, grey) and TRBJ (top, blue) combinations assessed by TCR sequencing of TCRab chains in whole blood of MIS-C patients. The relative frequency of all TRBVBJ combinations have been calculated per sample on the full TRB repertoire data. Combinations using TRBV11-2 are highlighted in red. Each red line indicates pairing with a given TRBJ, the thickness indicates the frequency of this pairing. The percentage values under each chart indicate the percentage of clonotypes composed with the TRBV11-2 gene. In (E-G) the CDR3 length distribution of clonotypes using TRBV11-2 is shown as

an histogram graph. Each clonotype is represented as a grey line. The thickness of the line represents the frequency of the clonotype within each repertoire. Since most of the clonotypes are not abundant, all the grey lines are stacked together and appear as a unique grey bar, which reflect the lack of expansion. Expanded clonotypes identified as detailed in the method section are shown in red. In (F-G) the same four patients are shown during the MIS-C episode (F) and after resolution (G). **(H)** Frequency of V $\beta$ 21.3+ T cells at different time points during and after the MIS-C episode in different patients, as assessed by flow cytometry. N=11, as indicated in Table S2. **(I)** Annexin-V staining of T cells in the indicated patients groups. Results show the ratio of the Annexin-V fluorescence in V $\beta$ 21.3+ vs V $\beta$ 21.3- T cells. N=3-4 in each group. Statistics were calculated using the Mann-Whitney test.

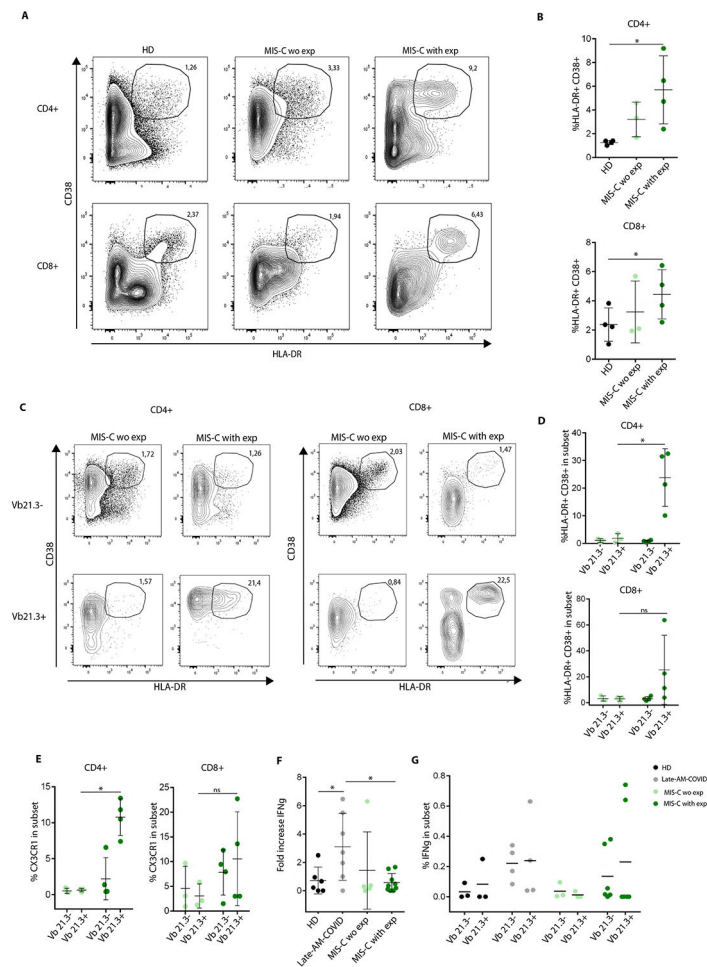


**Figure 4. T cell activation within V $\beta$ 21.3 and stimulation of T cells with viral peptides in vitro.** (A–D) Flow cytometry analysis of CD38 and HLA-DR expression in CD4 or CD8 T cells from the indicated patients’ groups (exp: V $\beta$ 21.3+ T cell expansion). (A) shows a representative staining, and (B) shows the mean  $\pm$ SD frequency of CD38+HLA-DR+ CD4 (top) and CD8 (bottom) T cells. N=3 to 4 per group, as indicated in Table S2; Statistical test: Mann-Whitney using FDR adjustment. (C–D) A V $\beta$ 21.3+ antibody was also included in the flow cytometry panel used in (A–B) allowing a specific comparison of the V $\beta$ 21.3– and V $\beta$ 21.3+ T cells in MIS-C patients. (C) shows a representative dot plot of CD38 and HLA-DR expression in the indicated subsets; (D) mean  $\pm$ SD frequency of CD38+HLA-DR+ in the indicated CD4 (top) and CD8 (bottom) T cell subsets. N=3 to 4 per group, as indicated in Table S2; Statistical test: Mann-Whitney. (E) Frequency of CX3CR1+ cells in gated V $\beta$ 21.3– and V $\beta$ 21.3+ CD4+ (left) and CD8+ (right) T cells in MIS-C without and MIS-C with expansion. (F) PBMCs from control, COVID-19 (adults, 6 months post infection) or MIS-C patients (with or without V $\beta$ 21.3+ T cell expansions) were stimulated for 6h with a commercial cocktail of synthetic peptides from S, N, and M SARS-CoV2 proteins in the presence of Golgi secretion inhibitors. Intracellular IFN $\gamma$  expression was then measured in T cells by flow cytometry. The fold increase was calculated as the ratio between the stimulated and the unstimulated conditions. N=5 to 9 per group, as indicated in Table S2;



Statistical test: Mann-Whitney using FDR adjustment. (G) shows the frequency of V $\beta$ 21.3+ and V $\beta$ 21.3- T cells expressing IFN- $\gamma$  after stimulation with S, N, M SARS-CoV2 peptides in the different patient groups as indicated (one dot: one patient).

**Table 1:**

Demographic and clinical data of pediatric patients with Kawasaki Disease or Toxic shock syndrome (*S.aureus* or *S. pyogenes*) and adult patients with mild or severe COVID-19

	pediatric COVID-19	children with Kawasaki Disease	children with Toxic shock syndrome ( <i>S.aureus</i> )	children with Toxic shock syndrome ( <i>S.pyogenes</i> )	adult with mild COVID-19	adult severe COVID-19
	N=11	N=16	N=39	N=19	N=21	N=10
<b>Age (y), median [Min-Max]</b>	2,5 [0,1-17,6]	2,9 [0,1-15,8]	14,7 [0,4-18]	4,1 [0,7-18]	42 [29,2-57,3]	60,8 [42,3-78,8]
<b>Female gender</b>	3 (27%)	9 (56%)	29 (74%)	10 (67%)	18 (86%)	5 (50%)
<b>ICU admission</b>	3 (27%)	3 (18%)	36 (100%) (n=36)	19 (100%)	0 (0%)	10 (100%)
<b>Vasoactive medications</b>	0 (0%)	1 (6%)	19 (65%) (n=29)	15 (83%)	0 (0%)	3 (30%)